Detoxification of Organophosphate Poisoning Using Nanoparticle Bioscavengers

ARTICLE *in* ACS NANO · JUNE 2015

Impact Factor: 12.88 · DOI: 10.1021/acsnano.5b02132 · Source: PubMed

12 AUTHORS, INCLUDING:

Che-Ming Jack Hu

Academia Sinica

37 PUBLICATIONS **1,644** CITATIONS

SEE PROFILE

Brian Luk

University of California, San Diego

19 PUBLICATIONS **381** CITATIONS

SEE PROFILE

Pavimol Angsantikul

University of California, San Diego

6 PUBLICATIONS **22** CITATIONS

SEE PROFILE

Liangfang Zhang

Massachusetts Institute of Technology

49 PUBLICATIONS **2,751** CITATIONS

SEE PROFILE

Detoxification of Organophosphate Poisoning Using Nanoparticle Bioscavengers

Zhiqing Pang,[†,‡] Che-Ming J. Hu,[†] Ronnie H. Fang,[†] Brian T. Luk,[†] Weiwei Gao,[†] Fei Wang,[†,‡] Erdembileg Chuluun,[†] Pavimol Angsantikul,[†] Soracha Thamphiwatana,[†] Weiyue Lu,[‡] Xinguo Jiang,[‡] and Liangfang Zhang*[,†]

[†]Department of NanoEngineering and Moores Cancer Center, University of California, San Diego, La Jolla, California 92093, United States and [‡]Department of Pharmaceutics, School of Pharmacy, Fudan University, and Key Laboratory of Smart Drug Delivery (Fudan University), Ministry of Education, Shanghai 201203, People's Republic of China

ABSTRACT Organophosphate poisoning is highly lethal as organophosphates, which are commonly found in insecticides and nerve agents, cause irreversible phosphorylation and inactivation of acetylcholinesterase (AChE), leading to neuromuscular disorders *via* accumulation of acetylcholine in the body. Direct interception of organophosphates in the systemic circulation thus provides a desirable strategy in treatment of the condition. Inspired by the presence of AChE on red blood cell (RBC) membranes, we explored a biomimetic nanoparticle consisting of a polymeric core surrounded by RBC membranes to serve as an anti-organophosphate agent. Through *in vitro* studies, we demonstrated that the biomimetic nanoparticles retain the enzymatic activity of membrane-bound AChE and are able to bind to a model organophosphate, dichlorvos, precluding its inhibitory effect on other enzymatic substrates. In a mouse model of organophosphate poisoning, the nanoparticles were shown to improve the AChE activity in the blood and markedly improved the survival of dichlorvos-challenged mice.

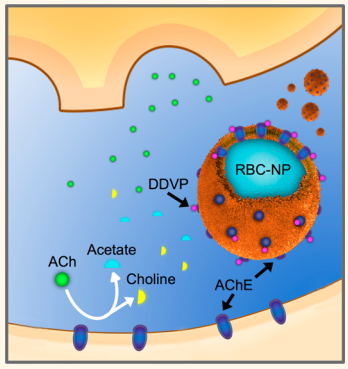

KEYWORDS: nanomedicine · biomimetic nanoparticle · biodetoxification · organophosphate · acetylcholinesterase

Organophosphate poisoning is caused by exposure to organophosphorus compounds (OPs), which irreversibly inactivate acetylcholinesterase (AChE) by phosphorylating the serine hydroxyl residue on AChE and lead to the accumulation of acetylcholine (ACh) in the body. Such accumulation disrupts cholinergic synaptic transmissions and can lead to various neurotoxic effects, including death in severe cases. OPs are one of the most common causes of poisoning worldwide and are frequently used in suicide attempts. There is an estimated 750 000 to 3 million global cases of OP poisonings per year, with hundreds of thousands of annual fatalities.[1,2] Because of their strong toxicity to humans, many OPs are applied in chemical warfare, serving as the primary ingredients in multiple nerve agents including sarin, tabun, soman, and VX. Typically, these nerve agents take effect within 1−10 min of exposure and can cause acute lethality within 15−30 min.[3] Combined with their ease of production, highly toxic OPs represent a great threat to both military and civilian populations.[4] Effective treatment of OP poisoning is of significant value to public health.

Removal of OPs from the body is difficult because they can easily enter circulation *via* several routes, including inhalation, ingestion, and dermal absorption. Current antidotes for OP poisoning consist of a pretreatment with carbamates to protect AChE from inhibition by OP compounds and postexposure treatments with anticholinergic drugs,[5] which serve to counteract the effects of excess ACh. Atropine is the most widely used antidote against OP poisoning in conjunction with pralidoxime or other pyridinium oximes (such as trimedoxime and obidoxime) for AChE reactivation.[6] However, these treatments are associated with serious side effects and can be difficult to administer. Recent meta-analyses indicate that the use of "-oximes" appears to be of no benefit and can potentially be detrimental.[7,8] In addition, it can be difficult to achieve a

* Address correspondence to zhang@ucsd.edu.

Received for review April 9, 2015 and accepted May 30, 2015.

Published online 10.1021/acsnano.5b02132

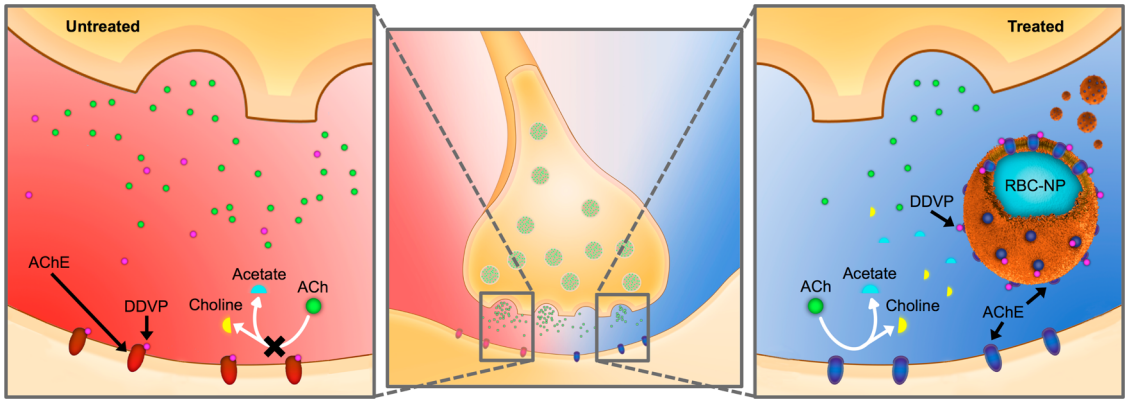

Figure 1. Schematic of RBC-NPs as anti-OP bioscavengers for treating OP poisoning. An idealized depiction of a neuronal synapse (center) under two opposing conditions. With no treatment (left), dichlorvos (DDVP), a model OP, irreversibly binds acetylcholinesterase (AChE), preventing the breakdown of acetylcholine (ACh) into choline and acetate. When RBC-NPs are introduced (right), they scavenge free DDVP molecules in circulation, preserving the ability of endogenous AChE at the synapse to perform the function of breaking down ACh.

sufficient level of atropinization,[9] as a high dose of the muscarinic antagonist is needed to block the action of overaccumulated peripheral ACh following AChE inactivation. Enzyme bioscavengers such as human serum butyrylcholinesterase (BChE) and human paraoxonase 1 (PON1) have been explored as treatment options to react and hydrolyze OPs before they can reach their physiological targets.[10−12] However, large-scale production of these recombinant proteins remains a hurdle in their translation.[13] Clinical treatment of OP poisoning may thus benefit from alternative strategies that can effectively deactivate the compounds in the bloodstream.

The activities of serum cholinesterases in the blood, which include both AChE and BChE, are the most widely used markers for diagnosing OP poisoning.[14] Whereas BChE exists primarily as a freely soluble form in the plasma, AChE is a membrane-anchored protein observed commonly on red blood cell (RBC) membranes, neuromuscular junctions, and cholinergic brain synapses. Recent advances in nanotechnology, particularly in cell-membrane-cloaked nanoparticles, have provided an opportunity for the membrane-bound AChE to be exploited for biomedical applications. It has been demonstrated that the cell-membrane-cloaking approach enables membrane proteins to be controllably anchored and displayed in a right-side-out manner on nanoscale particulates,[15−17] and the resulting biomimetic nanoparticles have been used for various biomedical functions, including bioscavenger applications for absorbing protein toxins and autoreactive immune factors.[15,18] It is conceivable that the platform may permit the systemic administration of cell-membrane-associated AChE to intercept toxic OPs in the bloodstream. To demonstrate OP detoxification using the biomimetic nanoparticles, herein, we prepared RBC membrane-cloaked nanoparticles (denoted "RBC-NPs") to exploit the RBC's surface AChE for OP scavenging (Figure 1). Dichlorvos (DDVP), one of the most widely used compounds in organophosphorus pesticides, is used as a model OP in this study. We showed that following cell membrane cloaking the RBC-NPs retain the membrane-bound AChE as well as their enzymatic activity. The biomimetic nanoparticles were applied as an OP scavenger to help maintain endogenous cholinesterase activity following OP exposure.

RESULTS

RBC-NPs were prepared according to a previously reported protocol in which purified RBC membranes were coated onto 100 nm poly(lactic-*co*-glycolic acid) (PLGA) polymeric cores *via* a sonication approach. To investigate the retention of AChE in the resulting RBC-NPs, Western blotting was conducted on RBC ghosts and RBC-NPs of equivalent membrane content. It was shown that following staining with anti-AChE antibodies RBC-NPs had banding patterns similar to those of RBC ghosts, including bands that correspond to monomers, dimers, and tetramers of the protein (Figure 2A). Total blotting intensity analyzed by ImageJ demonstrated that there was no statistically significant difference in the total blotting intensity between RBC ghosts and RBC-NPs, indicating efficient translocation of membrane proteins onto the nanoparticle substrates (Figure 2B). Further examination of AChE activity showed that RBC-NPs and RBC ghosts had largely similar AChE activity (Figure 2C). These results indicate that, after nanoparticle preparation, there was minimal loss of membrane-associated AChE content and little alteration in AChE enzyme activity, which is consistent with previous findings that demonstrated preservation of surface protein functionality on these cell-membrane-cloaked nanoparticles.[16,19] Given the well-studied reactivity between OPs and AChE, we then examined the effect of DDVP on the physicochemical properties of the RBC-NPs. Transmission electron microscopy (TEM) revealed that following mixing with

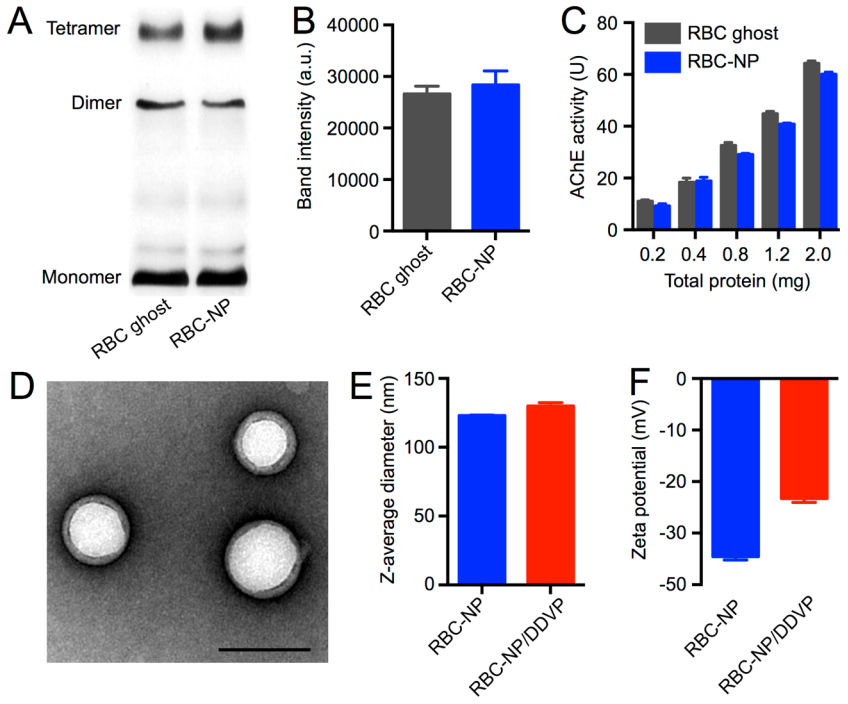

Figure 2. ***In vitro*** **characterization of RBC-NPs and RBC-NP/DDVP complexes. (A) Western blotting showing that RBC ghosts and RBC-NPs have similar blotting patterns following anti-AChE staining. (B) Quantification of Western blot band intensity showing that RBC ghosts and RBC-NPs contain equivalent amounts of AChE, indicating little loss of membrane-bound AChE during the RBC-NP preparation. (C) AChE activity test showing that RBC-NPs and RBC ghosts prepared from equivalent membrane content have similar AChE activity. (D) TEM image demonstrating the core/shell structure of the RBC-NP/DDVP complex. Scale bar = 100 nm. (E) Size and (F) surface ζ-potential of the RBC-NP and RBC-NP/DDVP complexes. All error bars represent standard error of mean.**

DDVP the RBC-NPs retained a core/shell structure that corresponds to unilamellar membrane coatings over the nanoparticle (Figure 2D). In addition, dynamic light scattering (DLS) measurements showed that RBC-NPs remained similar in size following DDVP exposure (Figure 2E), indicating that the DDVP reaction had little effect on the RBC-NPs' structure and stability. An increase in the particles' ζ-potential was observed following incubation with DDVP (Figure 2F), which can likely be attributed to the surface charge shielding effect by the bound DDVP molecules.

To investigate the ability of RBC-NPs to scavenge OPs, 0.4 and 0.1 mg of the particles suspended in 100 μL of aqueous solution was incubated with different concentrations of DDVP ranging from approximately 1 μg/mL to 1 mg/mL for 30 min. Following nanoparticle removal *via* centrifugation, the amount of nanoparticle-associated DDVP was quantified by measuring the remaining DDVP concentration in the supernatant *via* high-performance liquid chromatography (HPLC). It can be observed that RBC-NP/DDVP association occurs in a concentration-dependent manner (Figure 3A). A 4-fold increase in RBC-NP concentration correlated well with the observed right shift in absorption capacity, reflecting the 1:1 stoichiometry behind the covalent interaction between OPs and AChE. We also titrated RBC-NPs in a reaction mixture with 100 μL of aqueous solution and 5 μg of DDVP (Figure 3B). It was observed that to absorb 50% or 2.5 μg of DDVP approximately 32 μg of RBC-NPs was needed. A saturation level was reached as the RBC-NP concentration was increased above 1 mg/mL. To evaluate the specificity of DDVP removal by RBC-NPs, different nanoformulations, including 0.4 mg of RBC-NPs, PEGylated PLGA NPs (PLGA-PEG NPs), and PEG-liposomes, were incubated with 5 μg of DDVP for 30 min (Figure 3C). Almost all DDVP was removed by the RBC-NPs, whereas PLGA-PEG NPs and PEG-liposomes showed little DDVP removal, indicating that only RBC-NPs have the capacity to remove DDVP. Furthermore, *in vitro* AChE protection efficacy was evaluated by co-incubating RBC ghosts with increasing concentrations of DDVP in the presence of RBC-NPs (Figure 3D). Following 30 min of incubation, the RBC ghosts were isolated from the reaction mixtures and examined for AChE activity. It was observed that the DDVP concentrations required to inhibit 50% of the AChE activity on the RBC ghosts were 10, 43, and 312 μg/mL for the mixtures containing 0, 1, and 4 mg/mL of RBC-NPs, respectively. The increased retention of AChE activity on RBC ghosts validated the scavenging effect of RBC-NPs. Comparison of different nanocarriers' anti-OP effect was performed using 4 mg/mL of PLGA-PEG NPs, PEG-liposomes, and RBC-NPs incubated with 5 μg of DDVP and 2% of RBC ghosts in 100 μL of reaction mixture (Figure 3E). Following 30 min of incubation, isolated RBC ghosts were analyzed for their AChE activity. The RBC-NP group

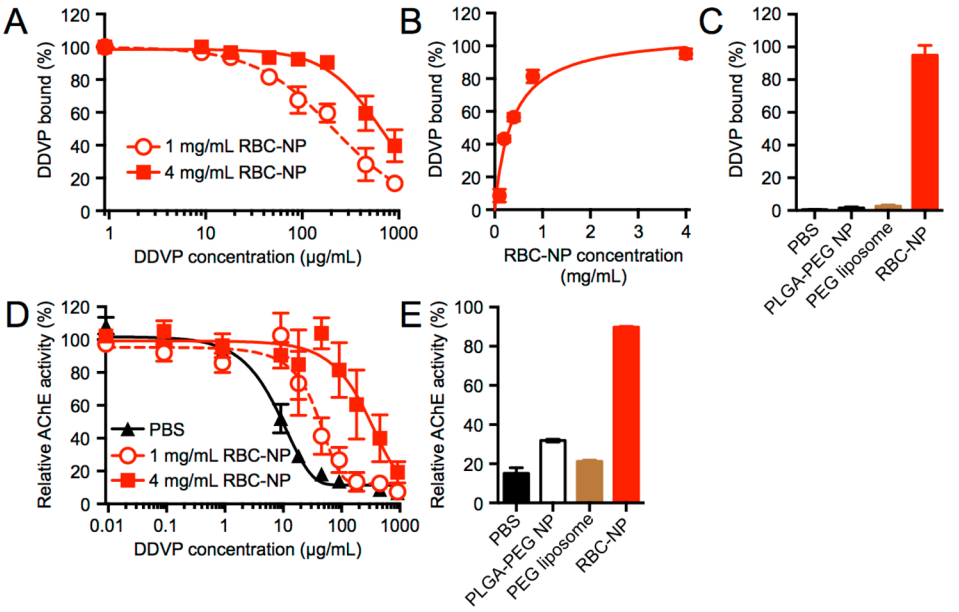

Figure 3. ***In vitro*** **neutralization of DDVP by RBC-NPs. (A) DDVP removal by different amounts of RBC-NPs was analyzed by titrating the concentration of DDVP in the reaction mixtures. (B) Kinetics of DDVP absorption and removal were investigated by incubating DDVP with different concentrations of RBC-NPs for 30 min. (C) DDVP absorption and removal by different nanoformulations (PLGA-PEG NPs, PEG-liposomes, and RBC-NPs) were analyzed by incubating DDVP with the respective nanoformulations for 30 min. (D) RBC ghost AChE activity in the presence of different concentrations of RBC-NPs following incubation with varying levels of DDVP for 30 min. Higher RBC-NP content conferred higher *in vitro* anti-OP effect. (E) RBC ghost AChE activity in the presence of different nanoformulations (PLGA-PEG NPs, PEG-liposomes, and RBC-NPs) following incubation with DDVP for 30 min. Co-incubation with RBC-NPs resulted in the highest AChE activity retention on the RBC ghosts. All error bars represent standard error of mean.**

showed AChE activity retention on the RBC ghosts significantly higher than that on the other nanoformulations. Approximately 90% of RBC ghosts' AChE activity was preserved in the presence of RBC-NPs, corroborating the receptor-specific anti-OP effect enabled by the biomimetic nanoparticles.

To examine the potential of RBC-NPs to detoxify DDVP *in vivo*, we used a mouse model of OP poisoning with either intravenous or oral administrations of DDVP. For intravenous DDVP administration, which obviated absorption variability, a lethal dose of DDVP (10 mg/kg) capable of inducing acute death in mice was injected *via* the tail vein. Mice in the treatment group received an intravenous injection of RBC-NPs or PLGA-PEG NPs at a dose of 200 mg/kg. It was shown that the mice without any treatment had a 100% mortality rate within 7 min after DDVP injection (Figure 4A). In the group treated with RBC-NPs, all mice survived the lethal DDVP challenge ($n = 10$, $p < 0.0001$). In contrast, PLGA-PEG NPs failed to improve the survival rate of the DDVP-challenged mice, and there was no significant difference in survival between the PLGA-PEG NP-treated group and the nontreatment group ($p = 0.3800$). Assaying the circulatory RBC AChE activity following the DDVP challenge and treatments further demonstrated that RBC-NPs significantly preserved RBC AChE activity as compared to the PLGA-PEG NP group ($p < 0.0001$) and the nontreatment group ($p < 0.0001$) (Figure 4B), whereas no statistical

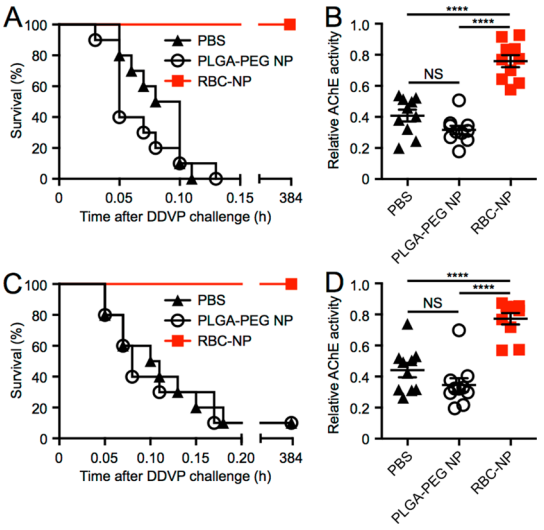

Figure 4. ***In vivo*** **neutralization of DDVP by RBC-NPs. (A) Survival curve of mice over 16 days and (B) relative RBC AChE activity of mice following intravenous administration of 200 mg/kg of RBC-NPs or PLGA-PEG NPs immediately after an intravenous injection of DDVP at a lethal dose (10 mg/kg) ($n = 10$). (C) Survival curve of mice over 16 days and (D) relative RBC AChE activity of mice following administration of 200 mg/kg of RBC-NPs or PLGA-PEG NPs immediately after oral administration of DDVP at a lethal dose (150 mg/kg) ($n = 10$). All error bars represent standard error of mean. ****$p \leq 0.0001$, NS = no statistical significance.**

significance was observed in the circulatory RBC AChE activity between the PLGA-PEG NP-treated group and

the nontreatment group (p = 0.0652). For the oral DDVP challenge, a scenario that models real-world exposure, mice were orally administered with a lethal dose of DDVP (150 mg/kg). Mice in the treatment group received an intravenous injection of RBC-NP or PLGA-PEG NP at a dose 200 mg/kg. It was shown that 90% of mice without any treatment died within 11 min after DDVP administration (Figure 4C). RBC-NP treatment remained beneficial to the overall survival with a 100% survival rate (p < 0.0001, n = 10), whereas PLGA-PEG NP treatment showed no survival advantage (p = 0.8989). The RBC AChE levels for the orally DDVP-challenged mice were consistent with the intravenously challenged ones. Whereas RBC-NP treatment resulted in significant RBC AChE activity retention in circulation as compared to the nontreatment group (p < 0.0001), no statistical significance in AChE activity was observed between the nontreatment group and the PLGA-PEG NP treatment group (p = 0.1479) (Figure 4D).

Recovery following DDVP poisoning was also investigated using circulatory RBC AChE activity as a marker (Figure 5A,B). It was shown that, by day 4, the RBC AChE activity returned to normal levels in those mice treated with RBC-NPs. This indicates the eventual clearance of OPs and the replenishment of cholinesterase content in circulation. To examine the *in vivo* fate of DDVP detoxified by RBC-NPs, the biodistribution of the RBC-NPs loaded with DDVP was studied. It was shown that the RBC-NP/DDVP complexes accumulated primarily in the liver (Figure 5C). Hematoxylin and eosin (H&E) stained liver histology on days 3 and 7 following the administration of RBC-NP/DDVP revealed normal hepatocytes supplied by blood vessels with no inclusion of Kupffer cells in the sinusoids (Figure 5D). The lack of liver tissue damage suggests that the sequestered DDVP was safely metabolized, showing minimal residual toxicity upon tissue distribution.

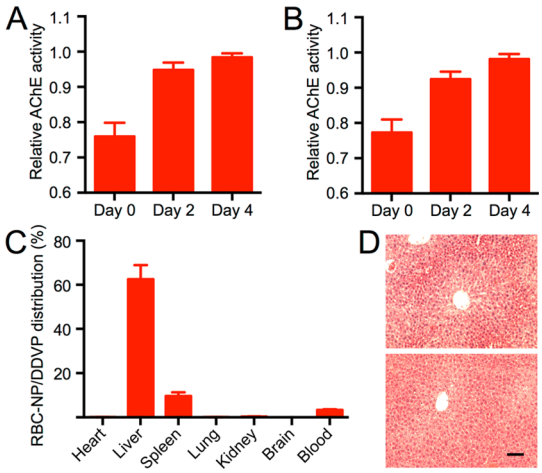

Figure 5. RBC AChE activity recovery following OP detoxification by RBC-NPs. (A) Relative RBC AChE activity recovered over a span of 4 days after the mice were challenged intravenously with DDVP (10 mg/kg) and immediately treated with RBC-NPs (200 mg/kg) (n = 10). (B) Relative RBC AChE activity recovered over a span of 4 days after mice were challenged orally with DDVP (150 mg/kg) and immediately treated with RBC-NPs (200 mg/kg) (n = 10). (C) Biodistribution of RBC-NP/DDVP complexes 24 h after intravenous injection. (D) Hematoxylin and eosin (H&E) stained liver histology showed no tissue damage on day 3 (top) and day 7 (bottom) following RBC-NP/DDVP complex injections. Each image is representative of five examined sections. Scale bar = 150 μm. All error bars represent standard error of mean.

DISCUSSION

OP poisoning remains a major public health issue as it is associated with high morbidity and mortality rates. Highly toxic OPs are considered one of the most dangerous chemical warfare agents and greatly threaten the safety of both military and civilian populations. OPs induce their acute toxicological effects through inhibition of AChE, which leads to an accumulation of ACh at synapses followed by overstimulation of cholinergic receptors and the disruption of neurotransmission. Deaths can occur within a few minutes after serious OP poisoning, which are generally due to respiratory failures mediated by several mechanisms. Paralysis of respiratory muscles resulting from failure of nicotinic ACh receptors is a primary cause of OP-induced lethality, and overstimulation of peripheral muscarinic receptors can also lead to choking due to excessive bronchorrhea and bronchoconstriction. Brain damage is another severe effect of OP intoxication as hydrophobic OPs readily cross the blood–brain barrier to exert their effects on the central nervous system. Therefore, anti-OP therapy needs to prevent OPs' pathophysiological effects in a direct and effective manner.

Currently, treatment of OP poisoning remains challenging.[20] Very few therapeutic options have been developed since the 1950s and 1970s, when anticholinergic drugs, carbamate-based pretreatment, pyridinium oximes, and benzodiazepines were introduced as anti-OP countermeasures in emergency situations.[21] Research on medical intervention against OP poisoning has been relatively static, with atropine, a standard antidote in the 1940s, remaining the primary anti-OP treatment. It is the only universally accepted treatment for muscarinic symptoms such as miosis, bronchospasm, vomiting, increased sweating, diarrhea, and urinary incontinence. However, despite its acceptance, there is no universal guideline on its administration and dosing. Under-dosing can delay optimal atropinization, resulting in death from central respiratory depression, hypoxia, and hypotension. Conversely, overdosing may lead to excessive anticholinergic toxicity, which can be fatal in severe cases.[22] Oximes are a unique class of anti-OP countermeasures, as they remove nerve agents from inhibited AChE to reactivate its activity. However, the efficacy of oxime therapy is still in debate. AChE inhibition by several nerve agents (*e.g.*, tabun and soman) has been shown to be irreversible

despite the application of clinically used oxime, as cholinesterases undergo rapid conversion into a non-reactivatable form upon phosphorylation.[23] Despite extensive research and development, there is not a single, broad-spectrum oxime suitable for antidotal treatment against all OP agents.[24]

Bioscavenger therapy has more recently emerged as a medical countermeasure to detoxify OPs in the bloodstream. These scavengers can be either stoichiometric (mole-to-mole neutralization) or catalytic (facilitating OP hydrolysis). PON-1, for instance, is the leading catalytic bioscavenger under development.[10,12] PON-1 is a calcium-dependent enzyme that hydrolyzes numerous OPs at a high efficiency.[25] Intravenous administration of purified PON-1 has been shown to protect guinea pigs against sarin and soman.[26,27] However, there are limitations regarding large-scale production and use of PON-1 as a therapeutic candidate. These include difficulties in producing recombinant PON-1 using microbial expression systems, low hydrolytic activity of wild-type PON-1 toward certain substrates, and low storage stability of the purified enzyme. HuBChE is another leading bioscavenger candidate. It is estimated that 200 mg of these stoichiometric anti-OP scavengers can protect a human against two times the LD_{50} dose of soman.[28] Animal studies in guinea pigs revealed that administration of large doses of HuBChE confer protection against up to 5.5 times the LD_{50} of soman or 8 times the LD_{50} of VX.[29] However, the lack of an affordable source of the enzyme remains a major hurdle in its translation. HuBChE isolation from human blood is economically prohibitive, and alternative production strategies using transgenic organisms pose immunogenicity concerns. Among other anti-OP candidates, AChE represents a promising bioscavenger with higher stereoselectivity than BuChE. Human AChE has been shown to more efficiently scavenge VX agents as compared to human HuBChE.[30,31] Unfortunately, development of AChE as a stoichiometric bioscavenger has been discontinued due to similar translational challenges.[21] Given this landscape, alternative strategies in developing OP bioscavengers can be of great therapeutic impact.

Nanoparticles have been developed rapidly over the past years due to their great potential in drug delivery. More recently, nanoparticles have been applied to remove toxins or chemicals from blood for biodetoxification.[32,33] To this end, little work has been done to apply nanoparticles as antidotes against OP poisoning. Here, we demonstrated that nanoparticles engineered with a biomimetic surface could be applied to intercept the binding between OPs and endogenous AChE, thereby reducing the severity of OP poisoning. Through the coating of cellular membranes, polymeric nanoparticles were successfully functionalized with enzymatically active membrane-bound proteins. The RBC-NPs demonstrated herein largely retained the content and functions of AChE on natural RBCs. These biomimetic nanoparticles were previously demonstrated to possess numerous cell-like functionalities, including long systemic circulation[16] and spontaneous interactions with membrane-active pathogenic factors.[15,18] The present study validates the potential of RBC-NPs as a novel form of anti-OP bioscavenger. The therapeutic potential of RBC-NPs was demonstrated using mouse models of OP poisoning *via* both intravenous and oral OP challenges. It was shown that the mortality rate was sharply reduced after treatment of RBC-NPs. In contrast, equivalent doses of PLGA-PEG NPs of analogous physicochemical properties failed to improve the survival rate of the DDVP-challenged mice, thereby reaffirming the unique functionality of RBC-NPs in anti-OP applications. Unlike existing anti-OP therapies that compete with ACh or block ACh receptors, the RBC-NPs function as an OP decoy and are thus less likely to induce anticholinergic side effects including ventricular fibrillation, dizziness, nausea, blurred vision, loss of balance, dilated pupils, photophobia, dry mouth, and extreme confusion. The entirely biocompatible and biodegradable nature of the platform also minimizes safety concerns associated with nanomaterial administration.

Toward future translation, the RBC-NP platform may present production advantages over other experimental bioscavenger platforms as purified RBCs are readily available in blood transfusion practices. It can be envisioned that blood-type-matched RBC-NPs may be administered to poisoned subjects for OP neutralization with minimal concerns of immunogenicity. In addition, as both nucleated and non-nucleated mammalian cell membranes have been demonstrated for the preparation of cell-membrane-cloaked nanoparticles,[16,34] other biomimetic nanoparticles with specific surface receptors may be prepared for different biodetoxification purposes. The unique bioscavenger approach using cell-membrane-cloaked nanoparticles may open a door to novel strategies in removing biological and chemical toxicants.

CONCLUSIONS

OP poisoning presents a major medical issue in the intensive care unit, and the acute nature of the poisoning demands effective therapeutic interventions. In this study, using DDVP as a model toxic agent, treatment of OP poisoning was demonstrated using RBC-NPs, which were capable of scavenging organophosphate compounds owing to the expression of functional membrane-bound acetylcholinesterase. The approach was shown to preserve endogenous RBC AChE activity *in vivo*, thereby validating its application in systemic OP neutralization. Rescue of mice following lethal OP toxin challenge was demonstrated using this nanoparticle bioscavenger approach, and the treated mice showed full AChE activity recovery and no observable liver injury following the treatment. As the platform consists of entirely biocompatible and biodegradable

materials, the biomimetic nanoparticles offer a promising strategy in treating acute OP poisoning resulting from exposure to a wide array of chemicals used in domestic, industrial, and military settings.

EXPERIMENTAL SECTION

Preparation of RBC-NPs and Characterization. RBC-NPs were prepared as previously described.[19] Briefly, 100 nm PLGA polymeric cores were prepared by a nanoprecipitation method. First, 0.67 dL/g carboxy-terminated 50:50 PLGA (LACTEL Absorbable Polymers) was dissolved in acetone at a concentration of 10 mg/mL. One milliliter of the PLGA solution was added rapidly to 2 mL of water and then placed in a vacuum to accelerate acetone evaporation. The resulting nanoparticle solution was mixed with CD-1 mouse RBC membrane vesicles and sonicated for 2 min using an FS30D bath sonicator at a power of 100 W. The fluorescence-labeled RBC-NPs were prepared using the same method except that 1,1′-dioctadecyl-3,3,3′,3′-tetramethylindodicarbocyanine perchlorate (DiD; excitation/emission = 644/665 nm; Life Technologies) was incorporated into the polymer solution at a concentration of 10 μg/mL during the nanoparticle core preparation. Note that all stated concentration values for RBC-NPs refer to the concentration of the PLGA polymer in the nanoparticle formulation. The RBC-NP/DDVP complex was prepared by mixing 100 μL of RBC-NPs (5 mg/mL) with 10 μL of DDVP (1 mg/mL) for 15 min. Particle size and ζ-potential of RBC-NPs and RBC-NP/DDVP complexes were determined by DLS measurements using a Malvern ZEN 3600 Zetasizer, which showed an average hydrodynamic diameter of 123 and 130 nm, respectively. The morphology of the RBC-NP/DDVP was examined with TEM after being stained with 1 wt % uranyl acetate.[16] As a control, DSPE-PEG(2000)-coated lipid−PLGA hybrid nanoparticles (PLGA-PEG NPs) were prepared through a nanoprecipitation method following a previously published protocol.[35] As another control, PEGylated liposomes (PEG-liposomes) consisting of 80 wt % of egg PC and 20 wt % of DSPE-PEG(2000)-methoxy (Avanti Polar Lipids) were prepared by a film hydration method as previously described.[36] Measured by DLS, the diameters of the PLGA-PEG NPs and PEG-liposomes were 117 and 105 nm, respectively.

Western Blotting of AChE and AChE Activity in RBC-NPs. RBC ghosts and RBC-NPs were prepared in SDS sample buffer (Invitrogen), and the total protein content in the samples was quantified by a Pierce BCA protein assay kit (Thermo). The samples were then resolved on a NuPAGE Novex 4−12% Bis-Tris 12-well gel in MOPS running buffer using the Novex SureLock X-cell electrophoresis system (Invitrogen). The samples were run at 165 V for 45 min. The proteins on the resulting polyacrylamide gel were then transferred to Protran pure nitrocellulose transfer and immobilization membrane (PerkinElmer) at 15 V for 30 min. After blocking with 5% fresh milk in PBST for 2 h at room temperature, the nitrocellulose membrane was incubated with monoclonal mouse anti-AChE (1:2000 diluted in 5% fresh milk in PBST; Abgent) overnight at 4 °C. After being washed with PBST three times, the nitrocellulose membrane was then incubated with goat anti-mouse IgG HRP conjugate (1:2000 diluted in 5% fresh milk in PBST; Millipore) for 2 h at room temperature. Afterward, the stained nitrocellulose membrane was subjected to ECL Western blotting substrate (Pierce) for 1 min and developed with a Mini-Medical/90 Developer (ImageWorks). Total blotting intensity was analyzed by ImageJ software to compare the AChE content between RBC-NPs and RBC ghosts. AChE activity in RBC-NPs and RBC ghosts was measured with an Amplex Red ACh/AChE assay kit (Invitrogen) using electric eel AChE as the standard.

DDVP Removal by RBC-NPs. To investigate the DDVP absorption and removal capability of RBC-NPs, 100 μL of PBS (1×, pH = 7.2) solution containing 4 or 1 mg/mL of RBC-NPs was incubated with 10 μL of different concentrations of DDVP for 30 min. Each sample was then spun down at 14 000 rpm in a Beckman Coulter microfuge 22R centrifuge for 10 min to pellet the nanoparticles. The free DDVP content in the supernatant was determined by using an HPLC system (Agilent 1100) with an analytical column (150 mm × 4.6 mm; pore size 5 μm; ZORBAX SB-C18; Agilent) at room temperature. The mobile phase consisted of a mixture of acetonitrile and water (50:50, v/v) at a flow rate of 1.0 mL/min. The sample injection volume was 10 μL, and the detector wavelength was 215 nm. The DDVP removal was calculated with the formula: DDVP removal (%) = (1 − DDVP in supernatant/total DDVP input) × 100%. All experiments were performed in triplicate. DDVP removal was plotted and fitted with the binding-saturation equation in GraphPad Prism. To investigate the effect of RBC-NP concentration on DDVP removal, 10 μL of PBS (1×, pH = 7.2) solution containing 5 μg of DDVP was incubated with 100 μL of solution containing different concentrations of RBC-NPs for 30 min. Each sample was treated as described above, and DDVP removal was calculated, plotted with DDVP concentration, and fitted with the binding-saturation equation. To compare the removal capability of different nanoformulations, 100 μL of PBS (1×, pH = 7.2) solution containing 4 mg/mL of RBC-NPs, PLGA-PEG NPs, or PEG-liposomes was incubated with 10 μL of solution containing 5 μg of DDVP for 30 min. Each sample was processed and analyzed as described above, and the DDVP removal was calculated.

***In Vitro* Anti-OP Effect by RBC-NPs.** *In vitro* anti-OP effect by RBC-NPs was investigated based on the AChE activity on RBC ghosts following co-incubation with RBC-NPs and DDVP. Briefly, 100 μL of PBS (1×, pH = 7.2) solution containing 2 μL of RBC ghosts and different concentrations of RBC-NPs was incubated with different concentrations of DDVP for 30 min. Each sample then was centrifuged at 2000 rpm in a Beckman Coulter microfuge 22R centrifuge for 10 min to selectively spin down the RBC ghosts, leaving RBC-NPs and DDVP in the supernatant. After the supernatant was discarded, the pellet of RBC ghosts was suspended in 10 μL of PBS and their AChE activity was measured by an Amplex Red ACh/AChE assay kit (Invitrogen). To compare the AChE protection effect by different nanoformulations, 100 μL of PBS (1×, pH = 7.2) solution containing 4 mg/mL of RBC-NPs, PLGA-PEG NPs, or PEG-liposomes was incubated with 10 μL of solution containing 5 μg of DDVP for 30 min. Each sample was spun down at 14 000 rpm in a Beckman Coulter microfuge 22R centrifuge for 10 min to remove the nanoformulations. The supernatant was added to 2 μL of RBC ghosts and incubated for 30 min. AChE activity on the isolated RBC ghosts was measured as described above.

***In Vivo* OP Detoxification by RBC-NPs Following Intravenous DDVP Challenge.** All animal experiments were performed in accordance with NIH guidelines and approved by the Institutional Animal Care and Use Committee (IACUC) of the University of California, San Diego. Animals were housed in a dedicated facility and were provided food/water *ad libitum*. RBC-NPs and PLGA-PEG NPs at a concentration 25 mg/mL suspended in 10% sucrose were first prepared. Six-week-old male CD-1 mice (Harlan Laboratories) were randomized to three groups of 10 mice. Each group of mice was intravenously administered with DDVP at a dose of 10 mg/kg through the tail vein. The treatment group received a tail vein intravenous injection of 200 mg/kg of nanoformulation immediately following the DDVP injection. The no treatment group was injected with DDVP only. Survival after DDVP injection was recorded, and statistical significance was determined using the log-rank test. For the no treatment group and the PLGA-PEG NP group, 50 μL of blood was collected by cardiac puncture immediately after death. For the RBC-NP group, 50 μL of blood was collected 1 h after DDVP injection by submandibular puncture. RBC ghosts were then derived from the collected blood based on a previously described protocol,[16] and the AChE activity of 10 μL of RBC ghosts was measured and compared to that of normal mice.

***In Vivo* OP Detoxification by RBC-NPs Following Oral Administration of DDVP.** RBC-NPs and PLGA-PEG NPs at a concentration 25 mg/mL suspended in 10% sucrose were first prepared. Six-week-old

male CD-1 mice were placed into three groups of 10 mice. Each group of mice was orally administered with DDVP at a dose of 150 mg/kg. The treatment group received a tail vein intravenous injection of 200 mg/kg of nanoformulation immediately after DDVP administration. The no treatment group was administered with DDVP only. Survival after DDVP administration was recorded, and statistical significance was determined using the log-rank test. For mice suffering from acute death and the PLGA-PEG NP group, 50 μL of blood was collected by cardiac puncture immediately after death. For surviving mice, 50 μL of blood was collected 1 h after DDVP administration by submandibular puncture. RBC ghosts were derived as previously described,[16] and the AChE activity of 10 μL of RBC ghosts was measured to compare with that of normal mice.

RBC AChE Activity Recovery after RBC-NP Treatment. After mice were challenged by intravenous or oral DDVP administration and treated with RBC-NPs, 50 μL of blood was collected on day 0, day 2, and day 4. RBC ghosts were derived from the collected blood, and the AChE activity of 10 μL of RBC ghosts was measured to monitor the recovery of AChE activity following RBC-NP treatment. Statistical significance was determined by a two-tailed *t* test.

Biodistribution of the RBC-NP/DDVP Complex. RBC-NP/DDVP complex was first prepared by mixing 5 mg of DiD-labeled RBC-NPs with 250 μg of DDVP. The mixture was subsequently filtered through a Sepharose CL-4B column to remove unbound DDVP. For the biodistribution study, 6-week-old male CD-1 mice were sacrificed 24 h after intravenous injection of the fluorescent RBC-NP/DDVP complex *via* the tail vein. The heart, liver, spleen, kidneys, lung, brain, and blood were collected and homogenized. The fluorescence of the homogenate at 665 nm with an excitation wavelength of 640 nm was read using a Tecan Infinite M200 multiplate reader. The resulting signal was then multiplied by the corresponding organ weight to obtain the total organ fluorescence, and the relative distribution of the RBC-NP/DDVP complex in each organ was calculated (n = 6). For the hepatotoxicity study, one group of mice was sacrificed on day 3 following the injection of the RBC-NP/DDVP complex and another group was sacrificed on day 7. The livers were collected, sectioned, and stained with H&E for histological analyses.

Conflict of Interest: The authors declare no competing financial interest.

Acknowledgment. This work is supported by the Defense Threat Reduction Agency Joint Science and Technology Office for Chemical and Biological Defense under Grant Number HDTRA1-14-1-0064 and by the National Institute of Diabetes and Digestive and Kidney Diseases of the National Institutes of Health under Award Number R01DK095168.

REFERENCES AND NOTES

1. Gunnell, D.; Eddleston, M.; Phillips, M. R.; Konradsen, F. The Global Distribution of Fatal Pesticide Self-Poisoning: Systematic Review. *BMC Public Health* **2007**, *7*, 357.
2. Eddleston, M.; Gunnell, D.; Karunaratne, A.; de Silva, D.; Sheriff, M. H.; Buckley, N. A. Epidemiology of Intentional Self-Poisoning in Rural Sri Lanka. *Br. J. Psychiatry* **2005**, *187*, 583–584.
3. Gupta, R. C. *Handbook of Toxicology of Chemical Warfare Agents*; Elsevier: London, 2009.
4. Yanagisawa, N.; Morita, H.; Nakajima, T. Sarin Experiences in Japan: Acute Toxicity and Long-Term Effects. *J. Neurol. Sci.* **2006**, *249*, 76–85.
5. Elsinghorst, P. W.; Worek, F.; Thiermann, H.; Wille, T. Drug Development for the Management of Organophosphorus Poisoning. *Expert Opin. Drug Discovery* **2013**, *8*, 1467–1477.
6. Jokanovic, M.; Prostran, M. Pyridinium Oximes as Cholinesterase Reactivators. Structure–Activity Relationship and Efficacy in the Treatment of Poisoning with Organophosphorus Compounds. *Curr. Med. Chem.* **2009**, *16*, 2177–2188.
7. Balali-Mood, M.; Shariat, M. Treatment of Organophosphate Poisoning. Experience of Nerve Agents and Acute Pesticide Poisoning on the Effects of Oximes. *J. Physiol. Paris* **1998**, *92*, 375–378.
8. Rahimi, R.; Nikfar, S.; Abdollahi, M. Increased Morbidity and Mortality in Acute Human Organophosphate-Poisoned Patients Treated by Oximes: A Meta-Analysis of Clinical Trials. *Hum. Exp. Toxicol.* **2006**, *25*, 157–162.
9. Karakus, A.; Celik, M. M.; Karcioglu, M.; Tuzcu, K.; Erden, E. S.; Zeren, C. Cases of Organophosphate Poisoning Treated with High-Dose of Atropine in an Intensive Care Unit and the Novel Treatment Approaches. *Toxicol. Ind. Health* **2012**, *30*, 421–425.
10. Nachon, F.; Brazzolotto, X.; Trovaslet, M.; Masson, P. Progress in the Development of Enzyme-Based Nerve Agent Bioscavengers. *Chem. Biol. Interact.* **2013**, *206*, 536–544.
11. Ceron, J. J.; Tecles, F.; Tvarijonaviciute, A. Serum Paraoxonase 1 (PON1) Measurement: An Update. *BMC Vet. Res.* **2014**, *10*, 74.
12. Rochu, D.; Chabriere, E.; Masson, P. Human Paraoxonase: A Promising Approach for Pre-treatment and Therapy of Organophosphorus Poisoning. *Toxicology* **2007**, *233*, 47–59.
13. Doctor, B. P.; Saxena, A. Bioscavengers for the Protection of Humans against Organophosphate Toxicity. *Chem. Biol. Interact.* **2005**, *157–158*, 167–171.
14. Worek, F.; Koller, M.; Thiermann, H.; Szinicz, L. Diagnostic Aspects of Organophosphate Poisoning. *Toxicology* **2005**, *214*, 182–189.
15. Hu, C. M.; Fang, R. H.; Copp, J.; Luk, B. T.; Zhang, L. A Biomimetic Nanosponge That Absorbs Pore-Forming Toxins. *Nat. Nanotechnol.* **2013**, *8*, 336–340.
16. Hu, C. M.; Zhang, L.; Aryal, S.; Cheung, C.; Fang, R. H. Erythrocyte Membrane-Camouflaged Polymeric Nanoparticles as a Biomimetic Delivery Platform. *Proc. Natl. Acad. Sci. U.S.A.* **2011**, *108*, 10980–10985.
17. Hu, C. M.; Fang, R. H.; Luk, B. T.; Zhang, L. Nanoparticle-Detained Toxins for Safe and Effective Vaccination. *Nat. Nanotechnol.* **2013**, *8*, 933–938.
18. Copp, J. A.; Fang, R. H.; Luk, B. T.; Hu, C. M.; Gao, W.; Zhang, K.; Zhang, L. Clearance of Pathological Antibodies Using Biomimetic Nanoparticles. *Proc. Natl. Acad. Sci. U.S.A.* **2014**, *111*, 13481–13486.
19. Hu, C. M. J.; Fang, R. H.; Luk, B. T.; Chen, K. N. H.; Carpenter, C.; Gao, W.; Zhang, K.; Zhang, L. 'Marker-of-Self' Functionalization of Nanoscale Particles through a Top-Down Cellular Membrane Coating Approach. *Nanoscale* **2013**, *5*, 2664–2668.
20. Hrabetz, H.; Thiermann, H.; Felgenhauer, N.; Zilker, T.; Haller, B.; Nahrig, J.; Saugel, B.; Eyer, F. Organophosphate Poisoning in the Developed World: A Single Centre Experience from Here to the Millennium. *Chem. Biol. Interact.* **2013**, *206*, 561–568.
21. Masson, P. Evolution of and Perspectives on Therapeutic Approaches to Nerve Agent Poisoning. *Toxicol. Lett.* **2011**, *206*, 5–13.
22. Eddleston, M.; Buckley, N. A.; Checketts, H.; Senarathna, L.; Mohamed, F.; Sheriff, M. H.; Dawson, A. Speed of Initial Atropinisation in Significant Organophosphorus Pesticide Poisoning—A Systematic Comparison of Recommended Regimens. *J. Toxicol. Clin. Toxicol.* **2004**, *42*, 865–875.
23. Thiermann, H.; Worek, F.; Kehe, K. Limitations and Challenges in Treatment of Acute Chemical Warfare Agent Poisoning. *Chem. Biol. Interact.* **2013**, *206*, 435–443.
24. Kassa, J.; Musilek, K.; Karasova, J. Z.; Kuca, K.; Bajgar, J. Two Possibilities How To Increase the Efficacy of Antidotal Treatment of Nerve Agent Poisonings. *Mini-Rev. Med. Chem.* **2012**, *12*, 24–34.
25. Masson, P.; Rochu, D. Catalytic Bioscavengers against Toxic Esters, an Alternative Approach for Prophylaxis and Treatments of Poisonings. *Acta Naturae* **2009**, *1*, 68–79.
26. Valiyaveettil, M.; Alamneh, Y.; Rezk, P.; Biggemann, L.; Perkins, M. W.; Sciuto, A. M.; Doctor, B. P.; Nambiar, M. P. Protective Efficacy of Catalytic Bioscavenger, Paraoxonase 1 against Sarin and Soman Exposure in Guinea Pigs. *Biochem. Pharmacol.* **2011**, *81*, 800–809.

27. Valiyaveettil, M.; Alamneh, Y. A.; Doctor, B. P.; Nambiar, M. P. Crossroads in the Evaluation of Paraoxonase 1 for Protection against Nerve Agent and Organophosphate Toxicity. *Toxicol. Lett.* **2012**, *210*, 87–94.
28. Ashani, Y.; Pistinner, S. Estimation of the Upper Limit of Human Butyrylcholinesterase Dose Required for Protection against Organophosphates Toxicity: A Mathematically Based Toxicokinetic Model. *Toxicol. Sci.* **2004**, *77*, 358–367.
29. Saxena, A.; Sun, W.; Fedorko, J. M.; Koplovitz, I.; Doctor, B. P. Prophylaxis with Human Serum Butyrylcholinesterase Protects Guinea Pigs Exposed to Multiple Lethal Doses of Soman or VX. *Biochem. Pharmacol.* **2011**, *81*, 164–169.
30. Cohen, O.; Kronman, C.; Raveh, L.; Mazor, O.; Ordentlich, A.; Shafferman, A. Comparison of Polyethylene Glycol-Conjugated Recombinant Human Acetylcholinesterase and Serum Human Butyrylcholinesterase as Bioscavengers of Organophosphate Compounds. *Mol. Pharmacol.* **2006**, *70*, 1121–1131.
31. Wandhammer, M.; Carletti, E.; Van der Schans, M.; Gillon, E.; Nicolet, Y.; Masson, P.; Goeldner, M.; Noort, D.; Nachon, F. Structural Study of the Complex Stereoselectivity of Human Butyrylcholinesterase for the Neurotoxic V-Agents. *J. Biol. Chem.* **2011**, *286*, 16783–16789.
32. Henry, B. D.; Neill, D. R.; Becker, K. A.; Gore, S.; Bricio-Moreno, L.; Ziobro, R.; Edwards, M. J.; Muhlemann, K.; Steinmann, J.; Kleuser, B.; et al. Engineered Liposomes Sequester Bacterial Exotoxins and Protect from Severe Invasive Infections in Mice. *Nat. Biotechnol.* **2014**, *33*, 81–88.
33. Leroux, J. C. Injectable Nanocarriers for Biodetoxification. *Nat. Nanotechnol.* **2007**, *2*, 679–684.
34. Fang, R. H.; Hu, C. M.; Luk, B. T.; Gao, W.; Copp, J. A.; Tai, Y.; O'Connor, D. E.; Zhang, L. Cancer Cell Membrane-Coated Nanoparticles for Anticancer Vaccination and Drug Delivery. *Nano Lett.* **2014**, *14*, 2181–2188.
35. Zhang, L.; Chan, J. M.; Gu, F. X.; Rhee, J. W.; Wang, A. Z.; Radovic-Moreno, A. F.; Alexis, F.; Langer, R.; Farokhzad, O. C. Self-Assembled Lipid-Polymer Hybrid Nanoparticles: A Robust Drug Delivery Platform. *ACS Nano* **2008**, *2*, 1696–1702.
36. Yang, D.; Pornpattananangkul, D.; Nakatsuji, T.; Chan, M.; Carson, D.; Huang, C. M.; Zhang, L. The Antimicrobial Activity of Liposomal Lauric Acids against *Propionibacterium acnes*. *Biomaterials* **2009**, *30*, 6035–6040.